defining J_{RT}

$$\Delta T = JT_B/r = J_{RT}/r = 0.12/r \quad (8)$$

where ΔT is in degrees celsius and r is in micrometers. For typical pore diameters of from 0.2 to 2 μm, therefore, the temperature differences required to maintain lubricant transport from reservoirs to their surroundings are from 0.6 to 0.06° C. Figure 2 is a graph of Eq. (7) for T = 300 K (26.8°C, 80.3°F).

Discussion

The lubricant transfer rate is governed largely by the geometry between the bearing and the reservoir and by the fashion in which the pores of various geometries are connected. The validity of the discussion is limited by the neglect of these parameters.

The important consequence of Eq. (7) is that it is first quantitative estimate of the temperature gradient necessary for a reservoir to function properly. The available temperature information, from satellites where such reservoir systems are used, indicates that some of the reservoirs are colder than the bearing area for a significant (if not major) part of the time. For such systems, one may justifiably question their utility.

If it is assumed that, to achieve reasonable transfer rates, the ΔT will be within a factor of 2 to 5 times that predicted by Eq. (7), i,e., about 2 to 4° F, further conclusions can be drawn. This temperature gradient is sufficiently small that the naturally occurring temperature gradients within the satellite could insure proper function. For such a configuration, it should be useful to construct reservoirs of high thermal conductivity materials.

In order to achieve a reasonable degree of predictability, the main source of variability, the pore size distribution, should be better defined. The only limitation is that the reservoir should not empty under the forces incurred during launch.

In summary, we have shown that the temperature of the reservoirs must be greater than that of the surroundings, but that the necessary temperature gradient can be quite small. The results also indicate that the most suitable reservoir material should have a high thermal conductivity and a near-homogeneous pore size distribution.

References

[1]Dormant, L. and Feuerstein, S., "Nylasint Pore System: Reservoir or Sink," *Journal of Spacecraft and Rockets,* Vol. 13, May 1976, pp. 306-309.

[2]Fote, A. A., Dormant, L., and Feuerstein, S., "Migration of Apiezon C on Metal Substrates Under the Influence of Temperature Gradients," TR-0076(6892)-1, Oct. 1975, the Aerospace Corporation, El Segundo, Calif. (to be published, *ASLE Lubrication Engineering*).

[3]Adamson, A. W., *The Physical Chemistry of Surfaces,* Academic Press, New York, 1969.

[4]Freeman, A.P., "Gyro Ball Bearings – Technology Today, *"Sixth AGARD Guidance and Control Meeting, Inertial Navigation – Components,* Braunschweig, Germany, May 1968.

Effect of Mass Asymmetry on Ballistic Match of Projectiles

Albert E. Hodapp Jr.*
Sandia Labs., Albuquerque, N. Mex.

Nomenclature

cg	= center of gravity
C_A	= axial force coefficient
C_{m_0}	= aerodynamic asymmetry induced pitching moment coefficient
$C_{M_{p\alpha}}$	= symmetrical Magnus moment slope coefficient (based on $d/2U$), 1/rad
$C_{M_q}+C_{M_{\dot\alpha}}$	= symmetrical pitch damping derivative coefficients (based on $d/2U$), 1/rad
C_{M_α}	= symmetrical pitching moment slope coefficient ($C_{M_\alpha}>0$ for shell), 1/rad
C_{n_0}	= aerodynamic asymmetry induced yawing moment coefficient
C_{N_α}	= symmetrical normal force slope coefficient, 1/rad
d	= body diameter (reference length), ft or m
i	$=(-1)^{1/2}$
I, I_X	= lateral and axial moments of inertia, respectively, slug-ft^2 or kg-m^2
J_{XY}, J_{XZ}	= products of inertia, slug-ft^2 or kg-m^2
m	= vehicle mass, slug or kg
p	= roll rate, rad/sec
q'	= dynamic pressure, lb/ft^2 or N/m^2
S	= reference area, ft^2 or m^2
S_g	= gyroscopic stability factor ($S_g>1$ necessary for stable flight)
t	= time, sec
U	= total velocity, fps
y_{cg}, z_{cg}	= body fixed lateral position of cg relative to origin of reference coordinate system, ft or m
α, β	= nonrolling angles of attack and side-slip, respectively, rad or deg
ξ	= complex total angle of attack relative to nonrolling coordinates, rad or deg

Subscripts

fm	= first maximum yaw
0	= conditions at muzzle exit ($t=0$)
1,2,3,4	= nutation, precession, trim, and yaw of repose, respectively

Received July 30, 1976. This work was supported by the U.S. Energy Research and Development Administration.

Index categories: LV/M Dynamics, Uncontrolled; LV/M Trajectories.

*Member of Technical Staff, Aerodynamics Department. Member AIAA.

Introduction

TO ballistically match similar artillery shells for identical muzzle exit conditions (i.e., make their mean impacts fall within some specified small range and deflection probable errors), it was shown by Vaughn and Wilson[1] that it is important to match the ballistic coefficients and yaw of repose induced drifts of the projectiles. Results presented herein indicate that in addition to these requirements it is necessary to control, within some permissible upper bound, the magnitude of the projectiles' initial angular motion. These initial disturbances can alter the flight path to produce trajectory deflections[2] and, through angle-of-attack induced drag, produce changes in ballistic coefficient. Both effects can result in unacceptably large relative range and/or deflection errors. The initial disturbances fall into two categories: 1) those introduced by the gun, which are usually small, and 2) those which result from projectile asymmetries. The latter category is investigated in this Note.

Small mass asymmetries (principal axis misalignment and lateral cg offset) inherent in certain artillery shells can have large effects on the magnitude of the projectiles' initial angular motion. It is shown herein that even when the fundamental ballistic similitude criterion is satisfied (i.e., the shapes, weights, moments of inertia, and static margins are matched) and identical muzzle exit conditions are achieved, a poor ballistic match can result when small differences in the level of principal axis misalignment and lateral cg offset exist between projectiles. The cg offset effect referred to here, which is indistinguishable from that of principal axis misalignment, is a gun twist dependent contribution to trim angle that is important for major caliber projectiles. This contribution, which has often been ignored in the past, is not to be confused with the better known cg offset induced

aerodynamic contribution that has a negligible influence on the trim angle of shells.

Analysis and Discussion

Making use of a nonrolling body fixed reference coordinate system (aeroballistic axes, Ref. 1) to develop the equations of motion, and assuming quasisteady conditions, small total angles of attack, symmetrical aerodynamic stability derivative coefficients, and equivalent lateral moments of inertia, the following description of the angular motion can be obtained.

$$\xi=\beta+i\alpha=K_1e^{(\lambda_1+i\omega_1)t}+K_2e^{(\lambda_2+i\omega_2)t}+K_3e^{ipt}+K_4 \qquad (1)$$

where

$$\lambda_{1,2}=\frac{1}{2}\left(\frac{q'S}{mU}\right)\left\{\left[\left(C_A-C_{N_\alpha}\right)+\left(\frac{md^2}{2I}\right)\left(C_{M_q}+C_{M_{\dot\alpha}}\right)\right](1\pm\tau)\mp 2\tau\left[\left(C_A-C_{N_\alpha}\right)-\left(\frac{md^2}{2I_X}\right)C_{M_{p\alpha}}\right]\right\}$$

$$\tau=1/\sqrt{1-1/S_g}$$

$$S_g=\left(\frac{pI_X}{2I}\right)^2\Big/\left(\frac{q'SdC_{M_\alpha}}{I}\right)$$ (Gyroscopic stability factor; $S_g>1$ for stable flight)

$$\omega_{1,2}=\left(\frac{pI_X}{2I}\right)\left[1\pm\sqrt{1-1/S_g}\right]$$

$$K_3=|K_3|\ (\sin\phi+i\cos\phi)$$

$$|K_3|=\left\{\frac{\left[\frac{\left[C_{m_o}+C_A(z_{cg}/d)\right]}{C_{M_\alpha}\eta^2}-\left(\delta_\alpha-\frac{py_{cg}}{U}\right)\left(1-\frac{I_X}{I}\right)\right]^2+\left[\frac{-\left[C_{n_o}-C_A(y_{cg}/d)\right]}{C_{M_\alpha}\eta^2}-\left(\delta_\beta+\frac{pz_{cg}}{U}\right)\left(1-\frac{I_X}{I}\right)\right]^2}{\left[\frac{I}{\eta^2}+\left(1-\frac{I_X}{I}\right)\right]^2+\left[\frac{\mu}{\eta}\right]^2}\right\}^{1/2}$$

$$\phi=\tan^{-1}\left\{\frac{\frac{-\left[C_{n_o}-C_A(y_{cg}/d)\right]}{C_{M_\alpha}\eta^2}-\left(\delta_\beta+\frac{pz_{cg}}{U}\right)\left(1-\frac{I_X}{I}\right)}{\frac{\left[C_{m_o}+C_A(z_{cg}/d)\right]}{C_{M_\alpha}\eta^2}-\left(\delta_\alpha-\frac{py_{cg}}{U}\right)\left(1-\frac{I_X}{I}\right)}\right\}+\tan^{-1}\left\{\frac{\frac{\mu}{\eta}}{\left[\frac{I}{\eta^2}+\left(1-\frac{I_X}{I}\right)\right]}\right\}$$

$$\eta=\sqrt{S_g}\left(\frac{2I}{I_X}\right),\qquad \eta\approx 20,\qquad \eta>>\mu$$

$$\mu=\left(\frac{q'S}{mU}\right)\left[\left(1-\frac{I_X}{I}\right)\left(C_A-C_{N_\alpha}\right)+\left(\frac{md^2}{2I}\right)\left(C_{M_q}+C_{M_{\dot\alpha}}+C_{M_{p\alpha}}\right)\right]\Big/\sqrt{\frac{q'SdC_{M_\alpha}}{I}}$$

$$\delta_\alpha=\frac{J_{XZ}}{(I-I_X)},\qquad \delta_\beta=\frac{J_{XY}}{(I-I_X)}$$

The complex constants K_1 and K_2, determined from the initial conditions, describe the initial magnitude and orientation of the transient nutation and precession vectors in the complex angle of attack plane. The trim angle K_3, which results from the asymmetries of the body, is described previously. The reader is referred to Ref. 1 for a description of the yaw of repose K_4.

Trim Angle

The principal difference between Eq. (1) and previously derived results, from which Refs. (3-5) are representative, is the more complete definition of the trim angle K_3. In addition to including the effects of aerodynamic asymmetries (C_{m_o} and C_{n_o}), the origin of the nonrolling reference coordinate system was laterally displaced from the *cg* (y_{cg} and z_{cg}), and products of inertia (J_{XY} and J_{XZ}) were included in the equations of motion [see Eq. (1)]. The direct contribution of the trim angle K_3 to angular motion is usually negligibly small; however, as shown later, small trim angles can have large effects on the magnitude of the initial transient angular motion (K_1 and K_2). Note in Eq. (1) that the lateral *cg* offsets (y_{cg} and z_{cg}) provide two basic contributions to K_3, the well-known aerodynamic effect ($C_A y_{cg}/d$, etc.), and an inertial effect (pz_{cg}/U, etc.) which has not been emphasized. For a gyroscopically stabilized slender projectile, $S_g>1$, $\eta>20$, and $\eta>>\mu$; therefore, the aerodynamic effects on trim are negligibly small in comparison to the inertial effects. The expression for trim angle magnitude [Eq. (1)] can be reduced to

$$|K_3|\approx\sqrt{\left(\delta_\alpha-\frac{py_{cg}}{U}\right)^2+\left(\delta_\beta+\frac{pz_{cg}}{U}\right)^2} \qquad (2)$$

Equation (2) indicates that principal axis misalignment (δ_α and δ_β) contributes directly to K_3, while the *cg* offset contribution is dependent on the ratio p/U, which in turn is dependent on the gun twist. Increasing the twist increases the *cg* offset contribution. Note that the magnitude of K_3, Eq. (2), is dependent on the relative signs of δ_α and y_{cg} and δ_β and z_{cg}. Therefore in order not to exceed a specified maximum allowable trim magnitude, bounds must be placed on both principal axis misalignment and *cg* offset such that the worst possible combination does not exceed the allowable.

Trim Effects on First Maximum Yaw

Assuming the initial total angle of attack ξ_o, intial angular rate $\dot\xi_o$, trim angle K_3, and yaw of repose K_4† are all known, the initial magnitudes K_1 and K_2 of the total transient angle of attack are obtained from Eq. (1) and its derivatives as

$$K_1=\frac{\dot\xi_o-\xi_o(\lambda_2+i\omega_2)+K_3[\lambda_2-i(p-\omega_2)]+K_4(\lambda_2+i\omega_2)}{(\lambda_1-\lambda_2)+i(\omega_1-\omega_2)} \qquad (3)$$

$$K_2=\frac{\dot\xi_o-\xi_o(\lambda_1+i\omega_1)+K_3[\lambda_1-i(p-\omega_1)]+K_4(\lambda_1+i\omega_1)}{(\lambda_2-\lambda_1)+i(\omega_2-\omega_1)} \qquad (4)$$

†Initially K_4 is negligibly small.

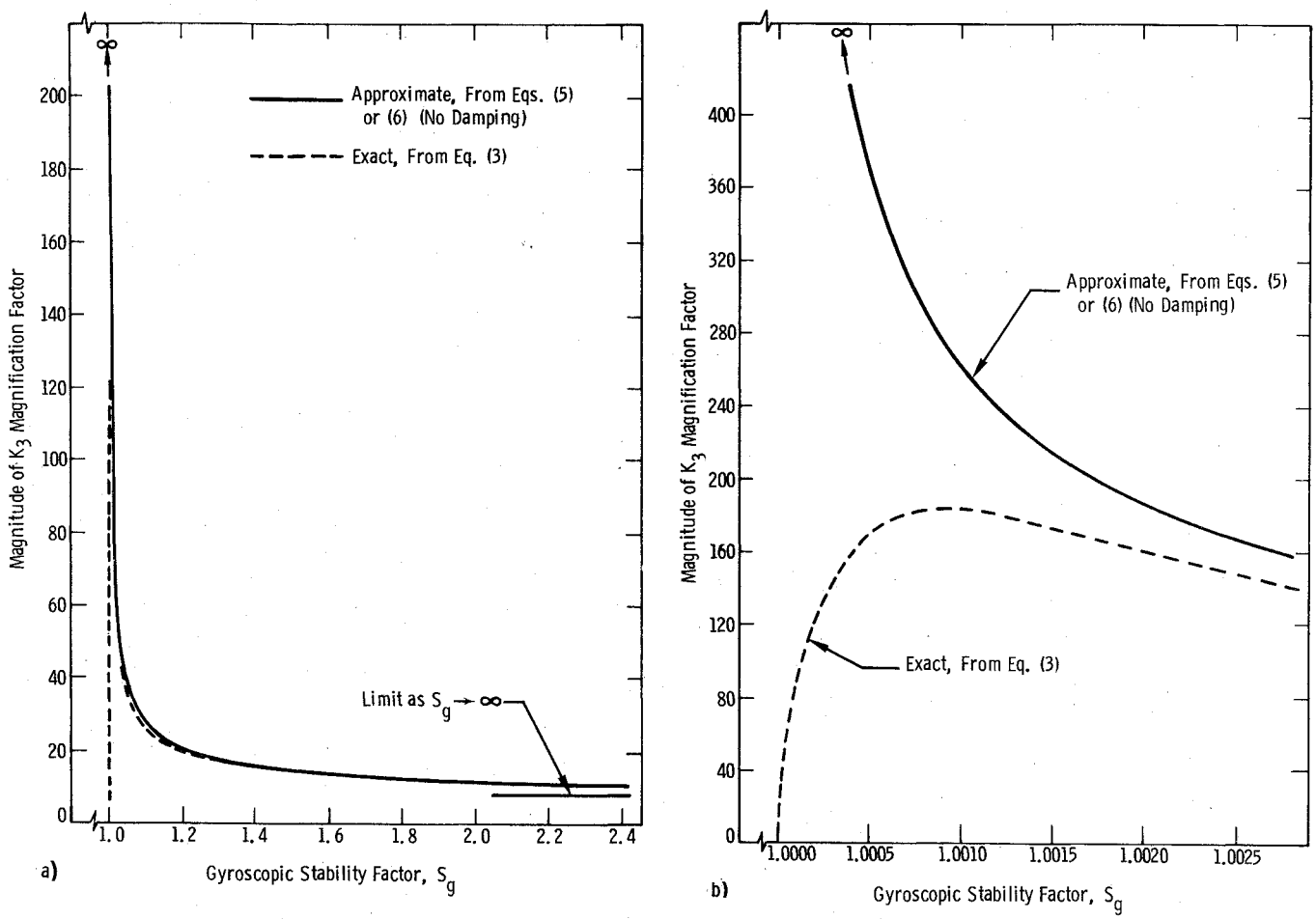

Fig. 1 Magnification of K_3 in K_1 or K_2; a) overall behavior; b) behavior near $S_g = 1$.

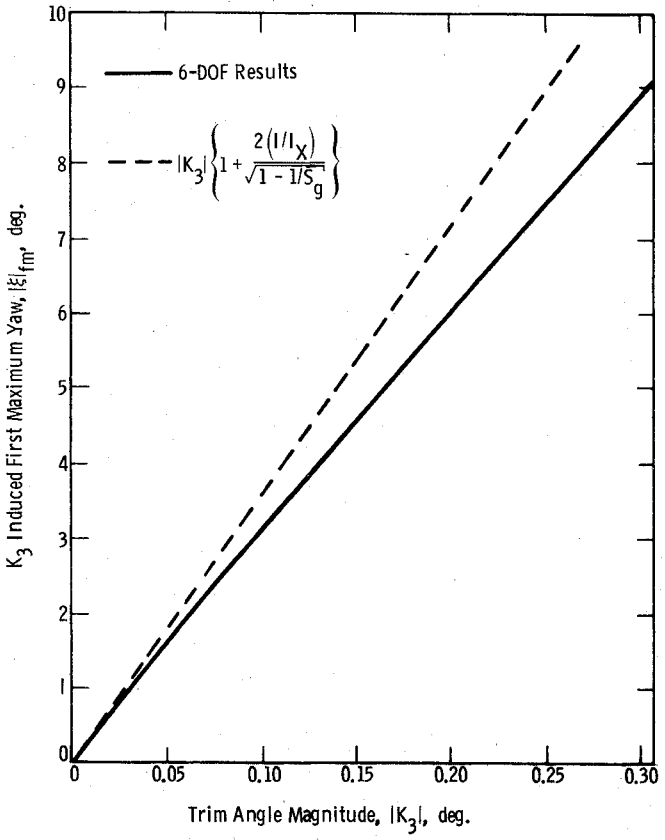

Fig. 2 Effect of K_3 on first maximum yaw.

The contributions of K_3 to K_1 and K_2, described in Eqs. (3) and (4), can either be enhanced or diminished by the remaining contributions. For a simple but accurate demonstration of the large effects that K_3 has on K_1 and K_2, the effects of damping and the contributions of $\dot{\xi}_0$, ξ_0, and K_4 will be ignored. Equations (3) and (4) then reduce to

$$K_1 \approx \frac{K_3(I/I_X)[1-(I_X/2I)\ (1-\sqrt{1-1/S_g})]}{\sqrt{1-1/S_g}} \approx \frac{K_3(I/I_X)}{\sqrt{1-1/S_g}} \tag{5}$$

$$K_2 \approx \frac{K_3(I/I_X)[1-(I_X/2I)\ (1+\sqrt{1-1/S_g})]}{\sqrt{1-1/S_g}} \approx \frac{K_3(I/I_X)}{\sqrt{1-1/S_g}} \tag{6}$$

Equations (5) and (6) show that the magnification of K_3 in K_1 and K_2 is approximately the same. The magnification factor (Fig. 1) is composed of two separate basic contributions. The first is the constant inertia ratio I/I_X of the numerator which contributes approximately a factor of ten magnification. The remaining S_g dependent contribution, provided by the denominator, produces a magnification factor which ranges from 1 for large S_g to an unbounded magnitude as $S_g \to 1$. Therefore, the product of these two contributions results in a magnification factor that is never smaller than I/I_X [Eqs. (5) and (6), Fig. 1a] As shown in Fig. 1a and 1b, where approximate and exact magnification factors are compared, the magnification factor contained in Eqs. (5) and (6) is an accurate approximation except for S_g values extremely close to 1 (within 10% down to $S_g = 1.003$). Instead of becoming unbounded at $S_g = 1$ (Fig. 1b) the effects of damping cause the magnitude of the magnification factor to

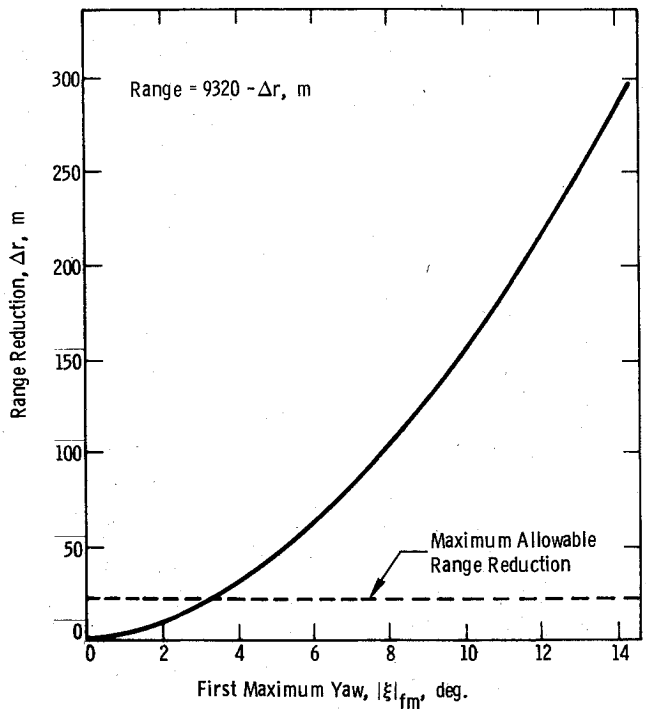

Fig. 3 Effect of first maximum yaw on range reduction.

reduce sharply to 0.5. Note in Fig. 1b that for this case the maximum magnification value occurs for $S_g = 1.0009$.

6-DOF Motion Simulations

To demonstrate the effects that K_3 has on the magnitude of the initial maximum total angle of attack (first maximum yaw), six-degree-of-freedom (6-DOF) flight simulations were obtained for an inertially asymmetric (principal axis misalignment and *cg* offset effects included) 8-in. artillery projectile. For a transonic low gyroscopic stability firing condition, the magnitude of K_3 was varied over the range 0 to 0.3 deg. With the exception of the asymmetries that produce K_3, all other physical characteristics of the projectile remained unchanged for the simulations. A perfect exit from the gun muzzle was assumed $\xi_0 = \xi_{\dot{0}} = 0$; therefore, the initial disturbances result from nonzero $\xi_{\dot{0}}$ caused by K_3.

The 6-DOF results presented in Fig. 2 confirm the large mangification of the trim angle in the initial transient angular motion. As shown, the analytical results provide an upper bound on the trim induced first maximum yaw ($|\xi|_{fm}$, Fig. 2). In addition to showing that small trim angles can produce very large initial disturbances, these results also indicate that small differences in the level of mass asymmetry between otherwise identical projectiles can have a large effect on the relative magnitudes of their initial angular motion.

For transonic firing conditions, damping is often extremely sluggish. Because of angle-of-attack induced drag and sluggish damping, the magnitude of the initial total transient angle of attack can have a relatively large effect on range through its effect on ballistic coefficient. This was found to have a much greater impact on the accuracy requirements than the trajectory deflections caused by the initial disturbances. For the selected transonic firing condition, the results presented in Fig. 3 demonstrate the large effect of induced drag on range. Note in Fig. 3 that reductions in range of 24, 60, and 138 m result for first maximum yaw values of 3.1, 6.0, and 8.9 deg. respectively. These first maximum yaw values were produced by K_3 values of 0.1, 0.2, and 0.3 deg (Fig. 2). All of these reductions in range exceed a 0.25% of range accuracy requirement, a representative requirement for ballistic similitude. These results indicate that small differences in the mass asymmetries of projectiles that are otherwise identical could result in failure to satisfy specified ballistic similitude requirements. Therefore the effects of small mass asymmetries must be considered when attempting to ballistically match projectiles.

Conclusions

Small mass asymmetries (principal axis misalignment and lateral *cg* offset) have proportionately large effects on the magnitude of artillery projectile first maximum yaw. The first maximum yaw levels produced by these asymmetries can cause unacceptable changes in range. After satisfying even the fundamental ballistic similitude criterion (identical shape, weight, static margin, and moments of inertia), it may still be necessary to reduce small differences in mass asymmetries between projectiles to insure ballistic similitude.

References

[1] Vaughn, H.R. and Wilson, G.G., "Effect of Yaw of Repose on Ballistic Match of Similar Projectiles," *AIAA Journal*, Vol. 9, June 1971, pp. 1208-1210.

[2] Figueras, R.I., "Influence of Dynamic Unbalance on Spin Stabilized Rockets," SAWE - Society of Aeronautical Weight Engineers, Inc., Paper 741, Los Angeles, Calif., May 1969.

[3] Nicolaides, J.D., "On the Free-Flight Motion of Missiles Having Slight Configurational Asymmetries," U.S. Army Ballistic Research Lab., Aberdeen Proving Ground, Md., Rept. 858, June 1953.

[4] Murphy, C.H., "Free Flight Motions of Symmetric Missiles," U.S. Army Ballistic Research Lab., Aberdeen Proving Ground, Md., Rept. 1216, July 1963.

[5] Vaughn, H.R., "A Detailed Development of the Tricyclic Theory," Sandia Labs., Albuquerque, N. Mex., SC-M-67-2933, Feb. 1968.

Launcher Length for Sounding-Rocket Point-Mass Trajectory Simulations

C. P. Hoult*
Windspeed, Inc., Los Angeles, Calif.

Introduction

THE simulation of sounding-rocket trajectories is basic to all other simulative exercises required for mission planning and hardware design. Because it is the cornerstone of all analytical efforts, large numbers of computer runs are required for this purpose.

Most of these simulations are made with a point-mass trajectory model in which the rigid-body rotational degrees of freedom are solved a priori, typically by assuming that the rocket always heads instantly into the relative wind. Such a model is extremely useful because it requires minimal effort in the preparation of input data, and because its running times and costs are low.

In reality, rockets have dynamical behavior corresponding to many modes associated with a large number of degrees of freedom. The point-mass trajectory model is a filtering approximation which tends to replicate the long period (Earth orbital period, if the rocket could pass through the solid Earth) or phugoid motion fairly well, while suppressing the dynamics of the short period motion, aeroelastic motions, etc., all of which have characteristic periods much shorter than the phugoid.

The point-mass model breaks down near the launch when the phugoid-short period intermodal coupling is especially large. The point-mass equations have a singularity there which is not present in the full set of six rigid-body equations.

Received April 12, 1976.
Index category: LV/M Dynamics, Uncontrolled.
*Consultant.